PHYSICAL REVIEW A **70**, 041802(R) (2004)

Hysteresis loop with controllable shape and direction in an optical ring cavity

Amitabh Joshi, Wenge Yang, and Min Xiao*
Department of Physics, University of Arkansas, Fayetteville, Arkansas 72701, USA
(Received 16 February 2004; published 14 October 2004)

We have experimentally observed a "backward" (clockwise rotating) hysteresis cycle in the system of an optical ring cavity containing three-level (Λ-type configuration) rubidium atoms. The shape and direction of the observed hysteresis cycles can be easily controlled with experimental parameters. Such an interesting phenomenon is caused by the greatly modified absorption, dispersion, and nonlinear optical properties of the three-level atomic medium, due to the induced atomic coherence.

DOI: 10.1103/PhysRevA.70.041802 PACS number(s): 42.65.Pc, 42.50.Gy, 42.65.Sf

The phenomenon of hysteresis is ubiquitous in magnetic, optical, electronic, mechanical, chemical, and biological sciences. A hysteresis cycle typically goes counterclockwise (noted as "forward") as experimentally demonstrated in many systems, such as ferroic materials [1], superconductors [2], spin glasses [3], semiconductors [4], polymers [5], porous media [6], granular systems [7], organic radicals [8], nanosystems [9], elastoplastic systems, and shape memory alloys [10]. The mechanisms for having such forward hysteresis cycles are different for different systems. For example, in ferromagnetic materials, the moving out of domain walls separating regions of antiparallel spins needs the increase of magnetic field, so the hysteresis (magnetization as a function of applied magnetic field) thus observed is a function of the work required to displace the domain walls, which ensures forward hysteresis cycles in such systems. In the system of two-level atoms contained in an optical resonator, the bistable curves in the input-output intensities are either due to the saturated absorption [absorptive optical bistability (OB)] or dispersion (dispersive OB) [4,11]. The appearance of the absorptive OB arises from the saturated absorption of the medium and the feedback effect due to the optical cavity, while the dependence of refractive index nonlinearly on the input intensity of the field is responsible for the dispersive OB. Simple arguments show that such OB curves should have forward hysteresis cycles, as observed previously [4,11].

Here, we report our experimental demonstration of a backward (clockwise) hysteresis cycle in a system of three-level (Λ-type) atoms, as shown in Fig. 1(a), inside an optical cavity. Using experimental parameters, such as coupling field frequency detuning, optical cavity detuning, and atomic number density, the shape and transition from a forward to backward hysteresis cycle can be well controlled. The controllability is provided by the unique abilities to manipulate the absorption, dispersion, and nonlinearity in such three-level atomic systems displaying electromagnetically induced transparency (EIT) owing to induced atomic coherence and quantum interference [12,13] among the atomic states, as well as the use of the optical cavity to provide the feedback mechanism [4,11]. Our study may act as a catalyst in search of such interesting behaviors in other systems exhibiting hysteresis (as listed in Refs. [1–10]), where appropriate physical mechanisms may be uncovered.

In optical science the hysteresis cycle is normally associated with optical bistable systems. Optical bistablities were studied in the late sixties [14]. The absorptive OB was predicted [15] in 1969 but any OB was experimentally observed in 1976 in sodium vapor [16]. Since then OBs are extensively studied in two-level atomic systems both theoretically and experimentally [4,11,17]. The underlying physical

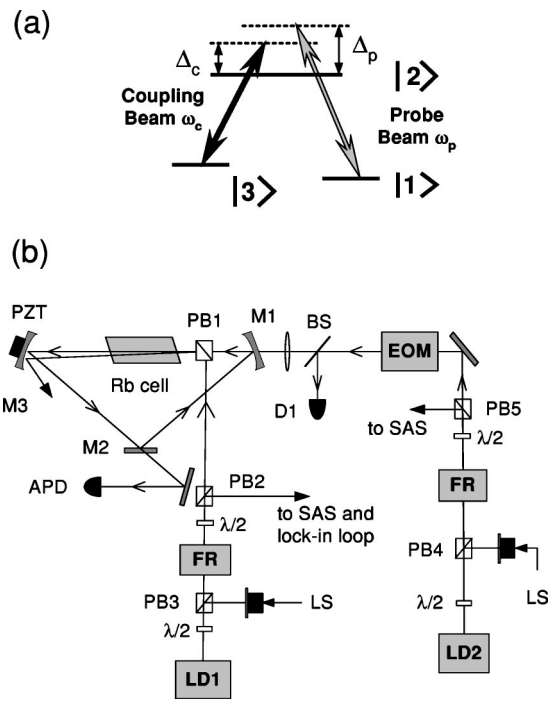

FIG. 1. (a) Diagram of the three-level atomic system. (b) The experimental arrangement used for studying optical bistability and optical multistability in ^{87}Rb atomic vapor: M1-M3 are mirrors of optical ring cavity; PZT is the piezoelectric transducer; LD1 and LD2 are coupling and probe lasers, respectively; PB1-PB5, polarizing cubic beam splitters; BS, beam splitter; EOM, electro-optic modulator; $\lambda/2$, half-wave plates; FR, Faraday rotator; D1, detector; APD, avalanche photodiode detector; LS, locking signal from reference Fabry–Perot cavity; and SAS is a saturation atomic spectroscopy set up.

*Email address: mxiao@uark.edu

mechanisms for the observed OB phenomena in two-level atomic systems has been well understood as the quantitative comparisons of the experimental results and the theoretical modeling were made [17]. In an earlier work [18] a mechanism for OB in three-level atomic systems with narrow nonabsorption resonance (related to EIT) was proposed. OB has also been observed in semiconductors (GaAs, InSb, etc.) and other materials [4,19]. A backward hysteresis cycle was observed in a two-level quantum-well system [20], which was explained to be caused by thermal effects. A partial backward hysteresis loop was theoretically predicted for the magnetic system with interface in a two-phase model, in which the phases were coupled antiferromagnetically [21]. Hamilton *et al.* [22] reported both forward and backward hysteresis loops in different parts of the same hysteresis cycle under optical pumping-based switch and saturation-based switching. In the work of Nalik *et al.* [23], multistable behavior (having both forward and backward hysteresis loops) was observed from combined effects of Zeeman pumping, electronic excitation, and birefringence of medium. However, these systems were complicated and the control (such as changing from forward to backward hysteresis) was difficult to achieve.

Controlling OB and optical multistability (OM) was demonstrated recently in three-level atoms inside an optical cavity [24,25], which sets the stage for studying the interesting backward hysteresis phenomenon in this system. The experiment was performed using the three-mirror optical ring cavity containing an atomic rubidium vapor cell with Brewster windows, which was heated to about 65–70 °C, as shown in Fig. 1(b). In order to shield the atoms from stray magnetic field, a μ-metal sheet was wrapped around the cell. The finesse of the optical cavity containing the atomic vapor cell was measured to be about 45 with a free spectral range of 822 MHz. To facilitate the scanning and locking of the optical ring cavity, one of the cavity mirrors was mounted on a piezoelectric transducer (PZT). The probe beam (ω_P, with spot size 80 μm) entered the cavity and circulated in it while interacting with the atomic transition $(\omega_{12}): 5^2S_{1/2}(F=1)$ (level$|1\rangle$) to $5^2P_{1/2}(F'=2)$ (level$|2\rangle$) of ^{87}Rb atom with probe-laser frequency detuning $\Delta_P=\omega_P-\omega_{12}$. The coupling beam (spot size about 700 μm) was injected into the cavity by a polarizing beam splitter so its polarization remained orthogonal to the probe laser. The coupling beam did not circulate in the cavity and it interacted with the atomic transition $(\omega_{23}): 5^2S_{1/2}(F=2)$ (level $|3\rangle$) to $5^2P_{1/2}(F'=2)$ (level $|2\rangle$) of ^{87}Rb atom with coupling laser frequency detuning $\Delta_C=\omega_C-\omega_{23}$. The two Hitachi HL7851G tunable diode lasers were both temperature and current stabilized with extended cavity feedback. A saturation absorption spectroscopy (SAS) set up along with a Fabry–Perot (FP) interferometer were used to measure Δ_P and Δ_C. Another frequency stabilized diode laser was used to lock the frequency of the optical ring cavity. The triangular scan of the probe laser (or the cavity input field) was provided by an electro-optical modulator (EOM).

In order to observe OB/OM in the input-output intensity plot from the optical ring cavity we first set the probe-laser frequency near the desired atomic transition (ω_{12}) and tune the coupling laser to another transition (ω_{23}) of the Λ-type system so the EIT condition was satisfied. The cavity was scanned across its resonance by applying a ramp on the PZT mounted on an M3 mirror. The cavity transmission peaks are symmetric when the cavity field frequency is far off from the atomic transition frequency ω_{12}. These transmission peaks show asymmetry once the probe and the coupling laser fields are tuned near resonance, indicating enhanced Kerr nonlinearity in the system. Then, the optical cavity was locked to the reference laser and the EOM scanned the intensity of the cavity input field. The base width of triangular pulse was about 5 ms, which is much slower than the system response timings. The estimated population decay and coherence relaxation constants between the two ground states are 1 and 0.5 MHz, respectively. No OB was observed under the exact condition of $\Delta_P=\Delta_C=0$. By setting one or both of the detunings to be nonzero, and with a reasonable coupling power, we observed typical OB. At low Δ_C, typical absorptive OB appears, but as Δ_C or Δ_P is increased to a larger value, dispersive-type OB behavior shows up [24].

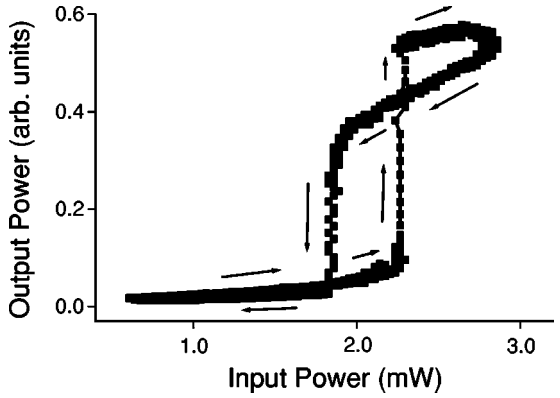

FIG. 2. Observed optical multistability in the input-output intensity characteristics of the system. The experimental parameters are $\Delta_P=0$ MHz, $\Delta_\theta=50$ MHz, $\Delta_C=137$ MHz, $T=65$ °C, and $P_C=14.0$ mW.

As Δ_C gets larger, a multistable hysteresis curve also appears [25], as shown in Fig. 2, which is obtained under the experimental conditions of $P_C=14.0$ mW, $T=65$ °C, Δ_θ (*the cavity detuning*)$=50$ MHz, $\Delta_C=137$ MHz, and $\Delta_P=0$. This hysteresis cycle has a topography of the Arabic-Roman numeral figure "eight." The arrows show the path taken by the cavity field intensity when the input intensity is scanned using the EOM. It is easy to see both the usual "forward" hysteresis loop (the lower one), as well as the "backward" loop (the upper one), in this composite hysteresis curve which is very different from previous studies [4,11,17,24,26].

Next, we show (in Fig. 3) how the width and the direction of the OB/OM hysteresis cycle can be efficiently controlled by varying only the coupling laser frequency detuning (Δ_C) while keeping all other experimental parameters fixed. Figure 3(a) essentially depicts the OB/OM hysteresis loop with all parameters the same as in Fig. 2, except with a lower Δ_C $(\Delta_C=103$ MHz). It represents a normal forward hysteresis cycle, where the upward switching threshold is higher in comparison to the downward switching threshold intensity. Hence, the main hysteresis cycle moves in the forward

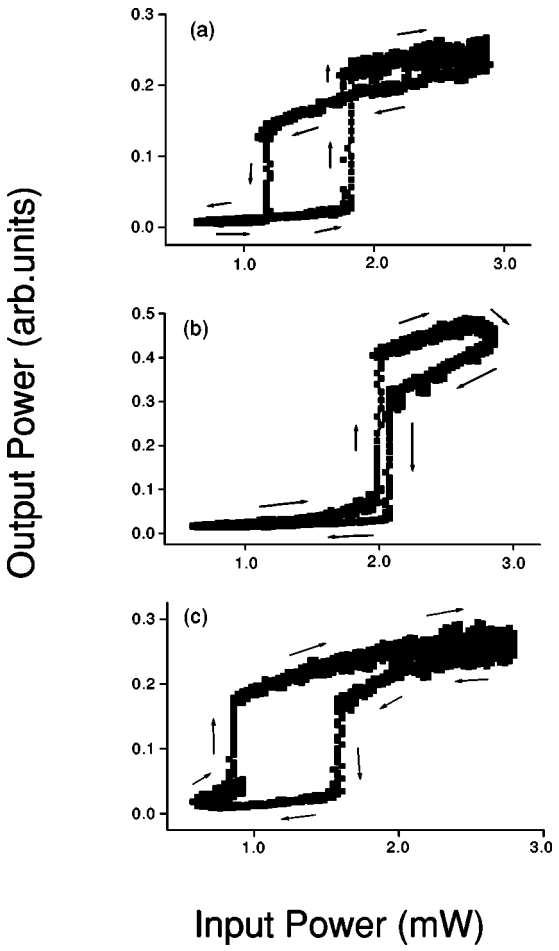

FIG. 3. The observed input-output intensity characteristics of the system. The parameters are $\Delta_P=0$, $\Delta_\theta=50$ MHz, $P_C=14.0$ mW, and $T=65$ °C, and (a) $\Delta_C=103$ MHz, (b) $\Delta_C=171$ MHz, (c) $\Delta_C=275$ MHz. As clearly seen, the hysteresis cycle changes shape and rotation direction as the coupling beam detuning increases.

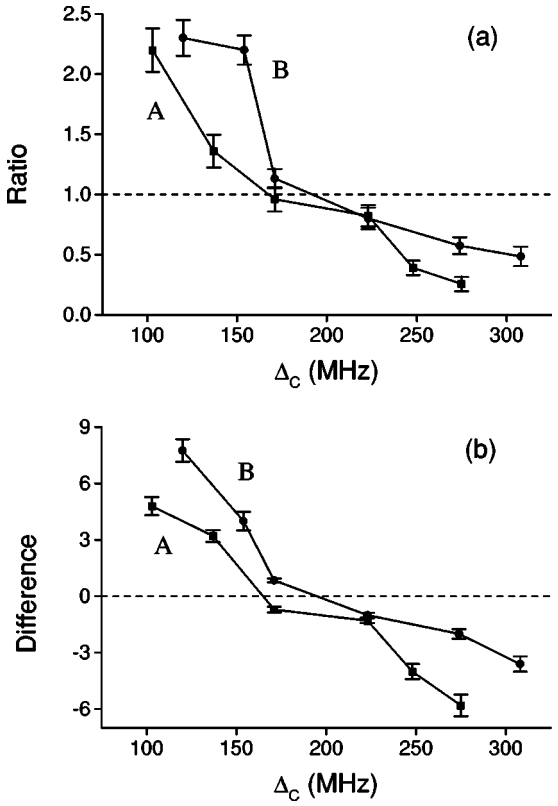

FIG. 4. (a) The ratio of upper to lower switching threshold intensities as a function of Δ_C with $\Delta_P=0$, $\Delta_\theta=50$ MHz, and $P_C=14.0$ mW. Curves A (■) and B (●) are for $T=65$ °C and $T=70$ °C, respectively. (b) Difference (in arb. units) upper to lower switching threshold intensities as a function of Δ_C with all other parameters the same as in (a).

(counterclockwise) direction. By increasing Δ_C further to the value of 171 MHz, the system exhibits dramatic changes in the width and the direction of the main hysteresis cycle [Fig. 3(b)]. The width of the OB/OM hysteresis cycle decreases considerably and now it moves in the backward (clockwise) direction, i.e., the upper switching threshold intensity becomes lower in comparison to the downward switching threshold intensity. Under a certain Δ_C value the two threshold intensities become identical and the main hysteresis loop disappears. The area enclosed within the hysteresis cycle is a measure of the energy dissipation in the system and here we can have a controllable and diminishing energy dissipation in the system with specially chosen parameters. In order to further expand the backward hysteresis cycle we increase Δ_C further to 275 MHz. By doing so, the width of the main hysteresis loop increases. While the upper switching threshold intensity goes down considerably, the downward switching threshold intensity goes up. Comparison of Figs. 3(a) and 3(c) clearly reveals that positions of upward and downward threshold values are reversed just by changing the coupling laser frequency detuning (Δ_C) alone while having all other system parameters fixed. Such behaviors can be exploited to make all-optical switching by alternating the coupling beam detuning (Δ_C) between two values, which can switch the cavity intensity between upper and lower branches. A similar transition from a forward to backward hysteresis cycle can also be seen by changing Δ_θ alone while keeping all other system parameters fixed. If the scanning is extended to a higher power level then the "beak" (the projected upper portion) of the hysteresis cycle keeps extending with power level, but the width and thresholds for up-jump and down-jump remain the same.

In order to have a better idea about how the upper and lower switching threshold intensities change with the coupling laser frequency detuning (Δ_C) we plot the ratio of upper switching threshold intensity to lower switching threshold intensity in Fig. 4(a) and the difference of these two quantities in Fig. 4(b), respectively, for two different temperatures. Clearly, both the ratio and difference of threshold intensities decrease as we increase the value of Δ_C. When the ratio (difference) crosses the magnitude of 1(0), it means that the hysteresis cycle reverses its direction. The ratio (difference) below the line of 1(0) indicates a backward hysteresis cycle. The shape and transition from forward to backward hysteresis cycles change when the atomic density (determined by the temperature of the atomic cell) is increased.

In the earlier OB experiment with a semiconductor me-

dium [20], where a 4.2-μm-thick GaAs etalon has been used at 80 K, the competition between electronic nonlinearity due to free exciton and the thermal effect makes the switching down intensity to be higher than the switching up intensity in the OB, which gives the backward hysteresis curve. In that experiment, the cavity detuning also played a significant role. Backward hysteresis was also observed in a cavityless OB system based on an optically induced absorption change due to thermal effect near the free and bound excitons in a CdS semiconductor system [27]. It is obvious that our current system is very different from those earlier observations of backward hysteresis, since thermal effects could not contribute to the atomic system. Since thermal effect is a very slow process, the current system will have more advantages in potential applications for all-optical switching and all-optical storage devices. Also, there were a lack of controls over the observed backward hysteresis cycles in the previous experiments due to the use of complicated systems. We expect that, as the coupling laser frequency detuning gets larger, Raman process starts to play an important role in the nonlinear interactions among laser fields and the three-level atomic medium, which can provide the energy needed for having the backward hysteresis observed in this system of EIT medium inside an optical cavity. Careful theoretical modeling is needed to have quantitative comparison with our experimental observations of the transition from forward to backward hysteresis cycles. We believe that Raman scattering may be a dominating process at a certain parametric value, and there could be interplay of EIT and this process in our system. Perhaps the more elaborated theory of density matrix based on a six-wave three-level Lambda model may turn out to be more appropriate for this purpose. Since the hysteresis cycle is closely related to the dissipation of the system, our current study could have implications to the recently proposed quantum information processing in such multilevel atomic assembles [28].

We acknowledge the funding supports from the National Science Foundation and the Office of Naval Research.

[1] K. Aizu, J. Phys. Soc. Jpn. **27**, 387 (1969); V. K. Vadhawan, *Introduction to Ferroic Materials* (Gordan and Breach, UK, 2002).
[2] M. Tinkham, J. U. Free, C. N. Lau, and N. Markovic, Phys. Rev. B **68**, 134515 (2003).
[3] H. G. Katzgraber *et al.*, Phys. Rev. Lett. **89**, 257202 (2002).
[4] H. M. Gibbs, *Optical Bistability: Controlling Light with Light* (Academic, New York, 1985), and references therein.
[5] C. M. Schroeder, H. P. Babcock, E. S. G. Shaqfeh, and S. Chu, Science **301**, 1515 (2003).
[6] B. Coasne, A. Grosman, C. Ortega, and M. Simon, Phys. Rev. Lett. **88**, 256102 (2002).
[7] I. Felner *et al.*, Phys. Rev. B **67**, 134506 (2003).
[8] M. E. Itkis, X. Chi, A. W. Cordes, and R. C. Haddon, Science **296**, 1443 (2002).
[9] O. Pietzsch, A. Kubetzka, M. Bode, and R. Wiesendanger, Science **292**, 2053 (2001).
[10] See for example, Int. J. Non-Linear Mech. **37**(8), 1261–1459 (2002).
[11] L. A. Lugiato, in *Progress in Optics*, edited by E. Wolf (North Holland, Amsterdam, 1984), Vol. 21, p. 71.
[12] S. E. Harris, Phys. Today **50**(7), 36 (1997), and references therein.
[13] H. Wang, D. J. Goorskey, and M. Xiao, Phys. Rev. Lett. **87**, 073601 (2001).
[14] C. V. Heer and R. D. Graft, Phys. Rev. **140**, A1088 (1965); M. Sargent III, W. E. Lamb, Jr., and R. L. Fork, *ibid.* **164**, 450 (1967).
[15] A. Szöke, V. Daneu, J. Goldhar, and N. A. Kurnit, Appl. Phys. Lett. **15**, 376 (1969).
[16] H. M. Gibbs, S. L. McCall, and T. N. C. Venkatesan, Phys. Rev. Lett. **36**, 1135 (1976).
[17] L. A. Orozco, H. J. Kimble, A. T. Rosenberger, L. A. Lugiato, M. L. Asquini, M. Brambilla, and L. M. Narducci, Phys. Rev. A **39**, 1235 (1989); J. Gripp, S. L. Mielke, and L. A. Orozco, *ibid.* **56**, 3262 (1997).
[18] D. F. Walls and P. Zoller, Opt. Commun. **34**, 260 (1980).
[19] H. M. Gibbs, S. L. McCall, T. N. C. Venkatesan, A. C. Gossard, A. Passner, and W. Wiegmann, Appl. Phys. Lett. **35**, 451 (1979); J. P. Löwenau, S. Schmitt-Rink, and H. Haug, Phys. Rev. Lett. **49**, 1511 (1982); A. Tredicucci, Y. Chen, V. Pellegrini, M. Börger, and F. Bassani, Phys. Rev. A **54**, 3493 (1996); A. Joshi and M. Xiao, Appl. Phys. B: Lasers Opt. **B79**, 65 (2004).
[20] J. L. Jewell, H. M. Gibbs, S. S. Tarng, A. C. Gossard, and W. Wiegmann, Appl. Phys. Lett. **40**, 291 (1982).
[21] M. J. O'Shea and A.-L. Al-Sharif, J. Appl. Phys. **75**, 6673 (1994).
[22] M. W. Hamilton, W. J. Sandle, J. T. Chilwell, J. S. Satchell, and D. M. Warrington, Opt. Commun. **48**, 190 (1983).
[23] J. Nalik, W. Lange, and F. Mitschke, Appl. Phys. B: Photophys. Laser Chem. **B49**, 191 (1989).
[24] A. Joshi, A. Brown, H. Wang, and M. Xiao, Phys. Rev. A **67**, 041801(R) (2003).
[25] A. Joshi and M. Xiao, Phys. Rev. Lett. **91**, 143904 (2003).
[26] W. Harshawardhan and G. S. Agarwal, Phys. Rev. A **53**, 1812 (1996).
[27] M. Dagenais and W. F. Sharfin, J. Opt. Soc. Am. B **2**, 1179 (1985).
[28] M. Bajcsy, A. S. Zibrov, and M. D. Lukin, Nature (London) **426**, 638 (2003).